

Self-induced transparency in semiconductor quantum dots

Giovanna Panzarini,^{1,*} Ulrich Hohenester,^{2,†} and Elisa Molinari¹

¹*Istituto Nazionale per la Fisica della Materia (INFM) and Dipartimento di Fisica, Università degli Studi di Modena e Reggio Emilia, Via Campi 213/A, 41100 Modena, Italy*

²*Institut für Theoretische Physik, Karl-Franzens-Universität Graz, Universitätsplatz 5, 8010 Graz, Austria*

(Received 24 September 2001; revised manuscript received 7 December 2001; published 8 April 2002)

We present a theoretical analysis of self-induced transparency in a sample of inhomogeneously broadened semiconductor quantum dots. A general theoretical framework accounting for mutual light-matter interactions in the presence of single and biexciton transitions is presented. Numerical results demonstrate that intense light pulses can propagate in realistic state-of-the-art dot samples without suffering strong losses.

DOI: 10.1103/PhysRevB.65.165322

PACS number(s): 42.50.Md, 78.67.Hc, 78.40.Pg

I. INTRODUCTION

Semiconductor quantum dots (QD's) are nanostructures which allow confinement of carriers in all three spatial directions,¹⁻³ resulting in discrete, atomiclike spectra and strongly enhanced carrier lifetimes. Such remarkable features make QD's similar to atoms in many respects, and suggest the exploitation of optically induced quantum coherence and correlations^{4,5} to drastically alter their nonlinear optical properties. Indeed, much recent work has been devoted to optically induced effects in QD's reminiscent of few-level systems: experimentally, coherent-carrier control of excitons⁶ or photon antibunching^{7,8} has been demonstrated, while theoretically, coherent population transfer,⁹ quantum-information processing,^{10,11} or the measurement of single scatterings¹² has been proposed.

Observation of optical coherence effects in ensembles of QD's is usually spoiled by inhomogeneous line broadening due to dot-size fluctuations, with typical broadenings comparable to the level splittings themselves. To overcome this problem, within the last couple of years a number of experimental techniques was developed to allow the observation of single quantum dots, thereby establishing the rapidly growing field of *single-dot spectroscopy*.¹³

It should be emphasized, however, that inhomogeneous line broadening leads to decoherence effects which are substantially different from those induced by homogeneous broadening.¹⁴ A light pulse propagating in a medium of inhomogeneously broadened QD's excites all the QD resonances *in phase*, where—at variance with the homogeneously broadened QD—each QD has a coherent time evolution. However, the phase varies from dot to dot, thus leading to interference effects, which in most cases prevent the observation of the coherent radiation-matter interaction. A striking exception is the phenomenon of *self-induced transparency* (SIT),^{4,15-19} a highly nonlinear optical coherence phenomenon which directly exploits inhomogeneous level broadening.

In their pioneering work McCall and Hahn^{15,16} first demonstrated that there exists a specific temporal pulse shape for which the light pulse entering a material of inhomogeneously broadened two-level systems propagates without suffering significant losses (“self-induced transparency”); this was indeed observed experimentally for atomic ensembles. SIT is important not only as a demonstration of quantum-

coherence-induced modifications of optical properties, but also as a prototypical example of a cooperative phenomenon: in this respect it differs from other coherent interactions such as Rabi oscillations, the ac Stark effect, and photon antibunching, which are essentially single-atom effects. Light-matter coupling plays a crucial role in SIT: its theoretical analysis not only requires considering the material response in the presence of the driving light pulse, but also the back action of the macroscopic material polarization on light propagation (through Maxwell's equations). In fact, it turns out that this light-matter interplay leads above a given threshold to a self-modulation of a laser pulse with arbitrary pulse shape. This is not the case in other coherent phenomena such as photonecho,^{20,21} where the modification of the external field acting on each dipole that is produced by all other dipoles can safely be ignored.

Quite generally, SIT is observable in any inhomogeneously broadened few-level system with sufficiently long-lived states. More specifically, for a laser pulse of duration τ_o the condition

$$T_{\text{mat}} \gg \tau_o \gg T^* \quad (1)$$

has to be fulfilled, where T_{mat} is the typical homogeneous lifetime of the two-level system, and $T^* = 1/\delta^*$ is a time associated to the inhomogeneous level broadening $\hbar \delta^*$. Thus, QD ensembles with their large inhomogeneous line broadenings and the long relevant coherence times⁶ are ideal candidates for a solid-state implementation of SIT. To the best of our knowledge, no work has been devoted yet to the study of SIT in semiconductor QD samples.

It is the purpose of the present paper to theoretically investigate self-induced transparency for an ensemble of semiconductor quantum dots. Here, the situation is more involved as compared to atoms, because a strong light pulse cannot only excite single electron-hole pairs (excitons) but also multiple pairs (multiexcitons). In this paper we will first develop a general theoretical framework suited for the description of light propagation in QD samples including exciton and biexciton transitions. Parameter estimates and numerical results for prototypical dot samples will be presented, which will demonstrate the feasibility of SIT in this class of materials.

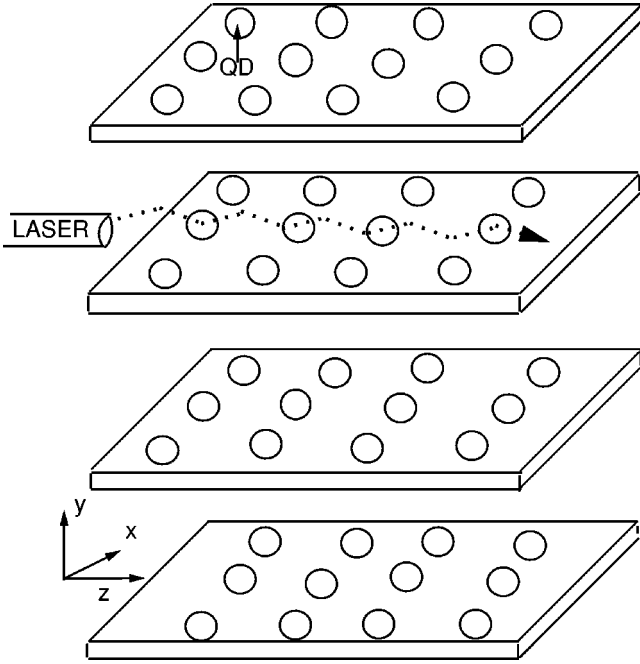


FIG. 1. Schematic representation of the model structure. It is formed by stacked layers of $\text{In}_x\text{Ga}_{1-x}\text{As}$ QD's (with different sizes) embedded in a GaAs host material, and is irradiated from the left-hand side by an intense laser beam propagating in the layer planes along z .

II. THEORY

A proper theoretical description of the mutual radiation-matter interaction requires the simultaneous solution of Maxwell's wave equation

$$\left(\nabla^2 - \frac{n^2}{c^2} \frac{\partial^2}{\partial t^2} \right) \mathbf{E} = \frac{4\pi}{c^2} \frac{\partial^2}{\partial t^2} \mathbf{P} \quad (2)$$

together with an equation describing the evolution of the QD system under the action of the electromagnetic field (we use cgs units throughout). The intense laser beam propagating along \hat{z} (see Fig. 1) is described by

$$\mathbf{E}(z,t) = \tilde{\mathcal{E}}(z,t) e^{-i(\omega_L t - k_L z)} \mathbf{u} + \text{c.c.}, \quad (3)$$

where \mathbf{u} is the polarization vector, ω_L the center-of-pulse frequency, and $k_L = n\omega_L/c$ the wave vector, with c the speed of light, and n the semiconductor refractive index. The interband polarization

$$\mathbf{P}(z,t) = \mathcal{P}(z,t) e^{-i(\omega_L t - k_L z)} \boldsymbol{\epsilon}_d + \text{c.c.} \quad (4)$$

is determined by all possible interband transitions occurring in the QD ensemble, with $\boldsymbol{\epsilon}_d$ the polarization vector. In Eqs. (3) and (4) $\tilde{\mathcal{E}}$ and \mathcal{P} are the envelope parts of the electromagnetic and polarization fields, respectively. Since different dots have different sizes, their energy levels are also dot-size dependent. Before arrival of the light pulse all quantum dots are assumed to be in their respective ground states $|0(\epsilon)\rangle$, where the dot-size-dependent exciton energy ϵ has been introduced to label dots with different sizes. However, cou-

pling to the light can induce transitions from $|0(\epsilon)\rangle$ to single and multiexciton states. Owing to condition (1), for a light frequency ω_L tuned to the ground-state exciton transition the QD states can be restricted to the spin-degenerate single-exciton ground states $|x(\epsilon)\rangle$ with frequency $\omega_x(\epsilon) = \epsilon$, and the biexciton ground state $|\lambda(\epsilon)\rangle$ with frequency $\omega_\lambda(\epsilon)$. For such a level scheme $\mathcal{P}(z,t)$ then reads

$$\begin{aligned} \mathcal{P}(z,t) = \mathcal{N} \sum_x \int g(\epsilon) d\epsilon [& M_{0x}(\epsilon) \rho_{x0}(\epsilon, z; t) \\ & + M_{x\lambda}(\epsilon) \rho_{\lambda x}(\epsilon, z; t)]. \end{aligned} \quad (5)$$

Here $g(\epsilon)$ is the normalized frequency distribution, \mathcal{N} is the uniform dot density, $\rho_{x0}(\epsilon, z; t) = \langle x(\epsilon) | \rho(z,t) | 0(\epsilon) \rangle$ and $\rho_{\lambda x}(\epsilon, z; t) = \langle \lambda(\epsilon) | \rho(z,t) | x(\epsilon) \rangle$ are the interband-polarization elements of the density matrix $\rho(z,t)$ in the rotating frame, and $M_{0x}(\epsilon) = e \langle 0(\epsilon) | \mathbf{r} | x(\epsilon) \rangle \cdot \boldsymbol{\epsilon}_d^*$ and $M_{x\lambda}(\epsilon) = e \langle x(\epsilon) | \mathbf{r} | \lambda(\epsilon) \rangle \cdot \boldsymbol{\epsilon}_d^*$ are the dipole elements for the exciton and biexciton transitions, respectively, which we assume to be parallel to each other (e is the electron charge).

The time evolution of the density matrix ρ of a specific dot is determined by the Liouville-von Neumann master equation which, within the rotating-wave approximation, reads^{12,22}

$$\frac{d\rho}{dt} = -\frac{i}{\hbar} (H_{\text{eff}} \rho - \rho H_{\text{eff}}^\dagger) + \Gamma_{\text{in}}[\rho]. \quad (6)$$

The effective Hamiltonian $H_{\text{eff}} = H_0 + H_R$ accounts for H_0 , the single-exciton and biexciton states (including a homogeneous lifetime broadening described by the phenomenological damping constants Γ_x and Γ_λ , which we assume to be independent of ϵ), and H_R , the light-dot coupling. More specifically, we obtain for a given z

$$\begin{aligned} H_0 = \hbar \sum_x \left[\left(\Delta_x(\epsilon) - i \frac{\Gamma_x}{2} \right) |x(\epsilon)\rangle \langle x(\epsilon)| \right. \\ \left. + \left(\Delta_\lambda(\epsilon) - i \frac{\Gamma_\lambda}{2} \right) |\lambda(\epsilon)\rangle \langle \lambda(\epsilon)| \right], \end{aligned} \quad (7a)$$

$$H_R = \frac{\hbar}{2} \sum_x [\Omega_{x0} |x(\epsilon)\rangle \langle 0(\epsilon)| + \Omega_{\lambda x} |\lambda(\epsilon)\rangle \langle x(\epsilon)|] + \text{c.c.}, \quad (7b)$$

with $\Delta_x(\epsilon) = \epsilon - \omega_L$, and $\Delta_\lambda(\epsilon) = \omega_\lambda(\epsilon) - 2\omega_L$ the exciton and biexciton detunings, and $\Omega_{x0}(z,t) = \mathcal{E}(z,t) M_{x0}(\epsilon)/\hbar$ and $\Omega_{\lambda x}(z,t) = \mathcal{E}(z,t) M_{\lambda x}(\epsilon)/\hbar$ the (time- and coordinate-dependent) exciton and biexciton Rabi frequencies, respectively [$\mathcal{E}(z,t) = \tilde{\mathcal{E}}(z,t) \mathbf{u} \cdot \boldsymbol{\epsilon}_d^*$]. Finally, the in-scattering term

$$\Gamma_{\text{in}}[\rho] = \sum_x [\Gamma_x \rho_{xx} |0(\epsilon)\rangle \langle 0(\epsilon)| + \frac{\Gamma_\lambda}{2} \rho_{\lambda\lambda} |x(\epsilon)\rangle \langle x(\epsilon)|] \quad (8)$$

ensures that in Eq. (6) the trace of the density matrix is preserved under the time evolution.

The small variation of $\mathcal{E}(z,t)$ over a wavelength and during an optical period allows us to simplify Maxwell's wave

TABLE I. Material and dot parameters used in our simulations.

Description	Value	Units
Dot density \mathcal{N}	8×10^{15}	cm^{-3}
Inhomogeneous broadening $\hbar\delta^*$ (FWHM)	25	meV
Biexciton binding $E_b(\epsilon)$	-2	meV
Exciton lifetime Γ_x^{-1}	100	ps
Biexciton lifetime Γ_λ^{-1}	50	ps
Optical matrix elements $M_{0x}, M_{x\lambda}$	2×10^{-17}	esu cm
Semiconductor refractive index n	3.3	

equation by performing the usual rotating-wave and slowly varying envelope approximation:^{4,23}

$$\left(\frac{\partial}{\partial z} + \frac{n}{c} \frac{\partial}{\partial t}\right) \mathcal{E}(z, t) \cong - \left(\frac{2\pi\omega_L}{nc}\right) \mathcal{I}\mathcal{P}(z, t). \quad (9)$$

The mutual interaction between radiation and matter relies on the fact that in Eq. (9) the polarization plays the role of the source for the electromagnetic (e.m.) field; meanwhile the e.m. field acts on the material system inducing the macroscopic polarization (4).

III. RESULTS

Next, we turn to the discussion of how an intense light pulse propagates in a sample of inhomogeneously broadened quantum dots. Our main emphasis will be focused on two points: first, the identification of those parameters determining the observation of SIT in a QD sample and second, the question of how the multiexciton QD level scheme modifies the usual two-level description of SIT.

In order to refer to a specific situation we will consider prototypical dot parameters (summarized in Table I). Figure 1 schematically depicts the proposed dot structure which is formed by stacked layers of $\text{In}_x\text{Ga}_{1-x}\text{As}$ QD's embedded in a GaAs host material, corresponding to samples currently grown by molecular-beam epitaxy by several groups;²⁴ an intense laser beam irradiates the sample from the left-hand side and propagates in the layer planes along z . This setup is chosen in anticipation of possible experimental realizations, where it might be more advantageous to place a few layers of QD's inside a waveguide structure rather than to grow QD layers as a volume material. We point out, however, that QD samples are currently grown by several different techniques, so that other types of QD's such as, e.g., dots grown by chemical self-aggregation techniques³ might be suited for experiment as well.

We shall make the usual assumption that light with well-defined circular polarization (helicity) creates electron-hole pairs (excitons) with well-defined spin orientations.^{2,23} Thus, for circular polarization \mathbf{u}_+ we recover an effective two-level system consisting of the ground state $|0\rangle$ and *one* exciton state (because both the second exciton state $|x_{\sigma_-}\rangle$ and the biexciton state $|\lambda\rangle$ can only be excited by photons with opposite helicity \mathbf{u}_-); in contrast, linearly polarized light couples together all states $|0\rangle$, $|x_{\sigma_+}\rangle$, $|x_{\sigma_-}\rangle$, and $|\lambda\rangle$. These simplified optical selection rules are chosen to allow us the

discussion of the two extreme cases of a pure two-level scheme and a maximally coupled three-level one; different situations, such as the one depicted in Fig. 1 (which approximately corresponds to linear polarization), are not expected to lead to qualitatively different results and will thus not be discussed explicitly.

Size fluctuations in the QD ensemble are accounted for by assuming a Gaussian distribution for the exciton resonances

$$g(\epsilon) = \frac{1}{\sqrt{2\pi\sigma}} \exp\left[-\frac{(\epsilon - \omega_L)^2}{2\sigma^2}\right] \quad (10)$$

centered around the mean dot frequency $\omega_o = \omega_L$; the variance σ is chosen to reproduce an inhomogeneous exciton and biexciton level broadening full width at half maximum (FWHM) of $\hbar\delta^* = 25$ meV, which corresponds to experimentally observed broadenings. In order for a pulse to propagate in a medium as if it were transparent, the radiation-matter interaction should be restricted to a time interval that is short compared to the phase memory time of the resonant material (i.e., to the homogeneous broadening time), and simultaneously that is large with respect to the inhomogeneous broadening time $1/\delta^*$, see Eq. (1), thus ensuring the same absorption coefficient for all Fourier components in the pulse. Since typical lifetimes in QD's are of the order of several tens of picoseconds,⁶ this condition can be satisfied using laser pulses with a duration of a few picoseconds (throughout our simulations we assume $1/\Gamma_x = 100$ ps; $1/\Gamma_\lambda = 50$ ps). The radiative lifetime in semiconductor QD's is related to the dipole moment M through the relation^{25,26}

$$\tau = \frac{3}{4n} \frac{\hbar c^3}{M^2 \omega^3}. \quad (11)$$

From the measured lifetimes $\tau = 1-2$ ns (Ref. 27) and assuming a pure radiative origin, we then take $M = M_{0x} = M_{x\lambda} = 2 \times 10^{-17}$ esu cm for our calculations. A uniform density $\mathcal{N} = 8 \times 10^{15} \text{ cm}^{-3}$ of QD's has been assumed throughout our simulations;²⁷ this value is a good compromise between the two opposite requirements of having no Coulomb coupling or tunneling between neighbor QD's, and of producing a large absorption coefficient in the structure. Finally, we choose a biexciton binding energy of $E_b = 2$ meV, irrespective of the QD size.

Figure 2 shows results of our simulations for the parameters listed in Table I. Let us first concentrate on the results for circular polarization, Figs. 2(a)-2(c), i.e., for the case in which our system behaves as an effective two-level system. It is apparent that the area theorem of McCall and Hahn is fulfilled in this situation. We recall that this theorem asserts that, for an ensemble of \mathcal{N} inhomogeneously broadened two-level systems with transition dipole moments M_{x0} , the pulse area, defined as

$$A(z) = \lim_{t \rightarrow \infty} \frac{M_{x0}}{\hbar} \int_{-\infty}^t d\bar{t} \mathcal{E}(z, \bar{t}), \quad (12)$$

satisfies the equation

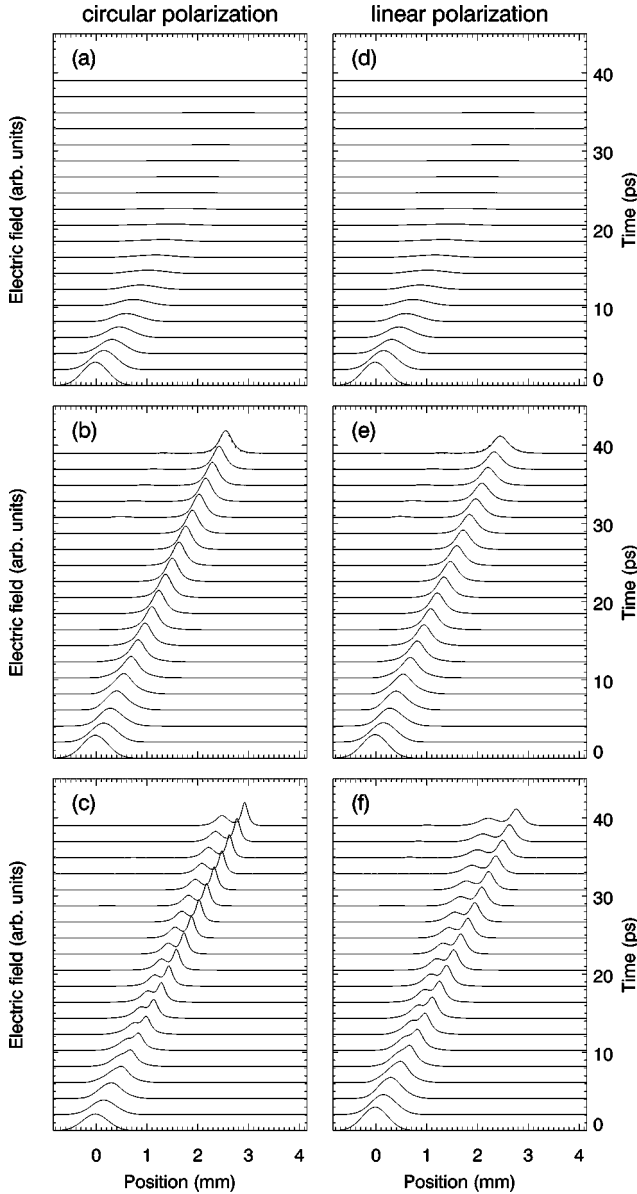


FIG. 2. Results of our simulations as described in the text and with the parameters listed in Table I. (a–c) [(d–f)] show the temporal evolution of the electric field for circular (linear) polarization, with the initial center-of-pulse strengths \mathcal{E}_o of (a) and (d) 6.7 kV/cm (area $A = 0.93\pi$), (b) and (e) 20 kV/cm ($A = 2.79\pi$), and (c) and (f) 33.4 kV/cm ($A = 4.65\pi$).

$$\frac{dA(z)}{dz} = -\frac{1}{2}\alpha \sin A(z) \quad (13)$$

when $\Gamma_x \rightarrow 0$, with the inverse of the absorption coefficient

$$\alpha = \frac{4\pi^2 \mathcal{N} \omega_L M_{x0}^2}{\hbar n c} g(\omega_L) \quad (14)$$

providing a characteristic length scale. [The demonstration of the theorem is easily obtained using the wave Eq. (9) together with the material (optical Bloch) Eq. (6)]. For a weak incident pulse one immediately observes from the linearized form of Eq. (13) that A decays according to

$\exp -1/2\alpha z$, as expected from Beer's law of linear absorption: within the framework of Bloch vectors,^{4,23} this decay is due to the small rotations of Bloch vectors out of their equilibrium positions and the resulting intensity loss of the light pulse. However, completely new features appear when $A \geq \pi$. Most important, if $A = m\pi$ ($m = 0, 1, 2, \dots$) the pulse area suffers no attenuation in propagating along z ; in fact each Bloch vector is now rotated from its initial state through a sequence of excited states back to the initial one, thus taking from the light field the same amount of energy that is given back. Moreover, areas that are even multiples of π are more stable than those that are odd multiples. In fact, either in the case of an incident pulse with initial area $(2m+1)\pi < A < 2(m+1)\pi$, or in the case with $2(m+1)\pi < A < (2m+3)\pi$ the propagation along z leads to a final stable area of $A = 2(m+1)\pi$.

We can now estimate the strength of the electric field and the thickness of the structure required for the observation of SIT in a typical QD sample as that of Fig. 1. The center-of-pulse field strength should be of the order of a few kV/cm to provide areas $A \sim \pi$ with a pulse duration of a few picoseconds, as required by Eq. (1);²⁸ the thickness of the sample should be of the order of a few millimeters, since for the prototypical parameters listed in Table I the characteristic length scale is $\alpha^{-1} \cong 0.15$ mm. Experimentally, it is certainly possible to grow macroscopic dot samples; furthermore, phenomena such as Rabi-type oscillations or self-induced transmission have been observed in a number of recent experiments in semiconductors of higher dimension.^{29–31}

In our simulations we perform in the wave Eq. (9) and the material Eq. (6) a real-space discretization z_i (with a mesh of typically 1000 points within a region of 5 mm), and in Eq. (6) a further detuning discretization Δ_i for excitons and biexcitons, respectively (60 points in a region of ± 5 meV). Equations (9) and (6) are then numerically integrated in time by use of standard library routines. We assume an initial Gaussian field profile $\tilde{\mathcal{E}}(z, t) = \mathcal{E}_o \exp\{-[(z-vt)^2/2\sigma_z^2]\}$, with $\sigma_z = 0.25$ mm (corresponding to a pulse duration of 2.75 ps). Instead of using a geometry where the light pulse enters from a dot-free region into the active dot region, we start from the beginning with a pulse propagating in the active region and turn on the material-light interaction quasiadiabatically over a time interval of 2 ps; such a quasiadiabatic turning on is necessary to suppress strong initial oscillations, and is expected to only influence field transients at early times.

At the lowest-field strength of Fig. 2(a) (corresponding to $\mathcal{E}_o \approx 6.7$ kV/cm and an area $A = 0.93\pi$) we observe that the field decays exponentially with z : in propagating through the medium, a fraction of the pulse energy is absorbed and retained as excitation energy of the QD's in the beginning length of the sample. This process progressively takes away energy from the pulse and determines its complete attenuation after a few absorption lengths. The situation is markedly different when $\mathcal{E}_o \approx 20$ kV/cm [Fig. 2(b)], which corresponds to an area $A = 2.79\pi$. The pulse loses initially some energy over a small number of absorption lengths; with a further increase of time (see axis on the right-hand side) and

penetration depth, however, it becomes compressed, and reaches the stable form of a 2π hyperbolic secant function of time and distance $\mathcal{E}(z,t) \propto 1/\cosh[(t-z/V)/\tau_f]$ (see dotted line in Fig. 1 at 40 ps, indistinguishable), with V the group velocity and τ_f a measure of the pulse duration.³² At such high intensities the leading edge of the pulse coherently drives the system in a predominantly inverted state; before dephasing processes take place, the trailing edge brings then the population back to the ground state by means of stimulated emission, and an equilibrium condition is reached in which the pulse receives through induced emission of the system the same amount of energy transferred to the sample through induced absorption.

Further increase to $A=4.65\pi$ [Fig. 2(c), with $\mathcal{E}_o \approx 33.4$ kV/cm] results in a *pulse breakup* into two peaks. Pulses with areas $2\pi < A < 3\pi$ becoming substantially shorter and more intense and reaching the final area of 2π with the stable hyperbolic secant shape, as well as pulse breakup for $A > 3\pi$, which had already been reported in the context of SIT in atomic ensembles; the present results strongly suggest that these features should be observable also with our QD ensemble.

For linearly polarized light more than two effective levels have to be considered, as previously discussed. Comparison of Figs. 2(a)–2(c) with 2(d)–2(f) reveals that our findings are not changed qualitatively in the presence of biexciton transitions. Again, for higher-field strengths one observes very stable pulse propagation, Figs. 2(e) and 2(f), and pulse breakup at the highest-field strength.

Finally, in Fig. 3 we plot for linear polarization the time evolution of the exciton Figs. 3(a)–3(c), and biexciton, Figs. 3(d)–3(f), populations, respectively, for a selected position of $z=2$ mm and for the same field strengths as in Fig. 2. Figure 3(b) clearly shows the oscillations of the exciton populations from zero to their maximum values and back to zero (i.e., 2π rotation of the Bloch vector); similarly, in Fig. 3(c) two oscillations can be resolved (i.e., 4π rotation). Note that the spectral width of the exciton-population transients is determined by the light-pulse duration τ_f . In general, the spectral width of the light pulse is sufficiently small to almost inhibit at zero detuning exciton-biexciton transitions, since the corresponding transition energy is redshifted as compared to $\hbar\omega_L$ because of Coulomb correlation effects³³ (biexciton binding of 2 meV in Table I). However, we infer from Figs. 3(e) and 3(f) that there is a more efficient biexciton-population channel through intermediate excitation of off-resonance excitons; at the field strengths investigated these biexcitons remain excited, thus leading to a small damping of the propagating light pulse. However, from Fig. 2 we observe that such damping has no significant impact on the pulse propagation along distances of the order of a few α^{-1} .

IV. SUMMARY

In conclusion, we have discussed the phenomenon of self-induced transparency in a semiconductor quantum dot sample with inhomogeneous level broadening. A general theoretical framework accounting for the mutual light-matter system in the presence of single- and multiexciton transitions has been developed. We have shown that for typical dot and material parameters SIT should be observable in state-of-the-

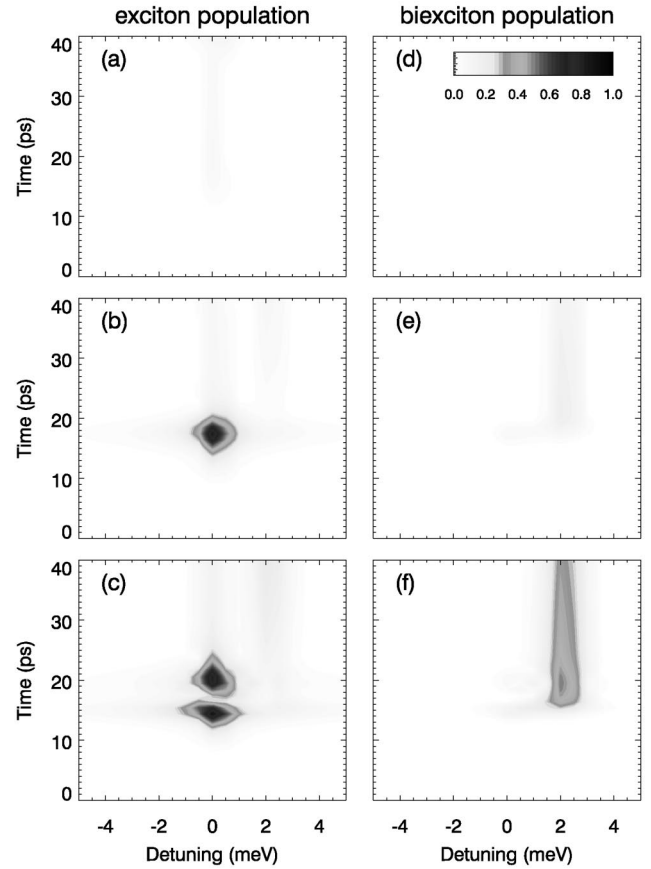


FIG. 3. Temporal evolution of the (a–c) exciton population $\Sigma_x \rho_{xx}(\epsilon, z; t)$ and (d–f) biexciton population $\rho_{\lambda\lambda}(\epsilon, z; t)$ at a distance $z=2$ mm, for linear polarization, and for electric-field strengths \mathcal{E}_o of (the same as in Fig. 1) (a) and (d) 6.7 kV/cm, (b) and (e) 20 kV/cm, and (c) and (f) 33.4 kV/cm; instead of ϵ we use $\hbar\Delta_x(\epsilon)$ and $\hbar\Delta_\lambda(\epsilon)$ for excitons and biexcitons, respectively.

art QD samples. Numerical simulations have revealed that the qualitative behavior of SIT is not changed in the presence of biexciton transitions, and only slightly higher-energy losses occur through the biexciton channel. SIT in QD samples constitutes a prototypical example for quantum coherence and for mutual light-matter coupling. It is expected to be of importance for the implementation of optically controllable switches or the propagation of intense laser pulses in high-density QD samples, which might be of relevance for QD-based laser devices.

ACKNOWLEDGMENTS

We are deeply grateful to Giovanna Panzarini, who introduced us to many aspects of semiconductor quantum optics and shared with us her physical intuition and her joy for the beauty of physics. She was physically fragile, but intellectually a strong and powerful woman, with a rich and attentive personality. Giovanna’s early death leaves us astonished and in deep pain. We will keep her in our hearts. This work was supported in part by the INFN through Grant No. PRA-99-SSQI, and by the EU under the TMR Network “Ultrafast Quantum Optoelectronics” and the IST program “SQID.”

- *Deceased October 23, 2001.
- [†]Electronic address: ulrich.hohenester@uni-graz.at
- ¹D. Bimberg, M. Grundmann, and N. Ledentsov, *Quantum Dot Heterostructures* (Wiley, New York, 1998).
- ²L. Jacak, P. Hawrylak, and A. Wojs, *Quantum Dots* (Springer, Berlin, 1998).
- ³U. Woggon, *Optical Properties of Semiconductor Quantum Dots* (Springer, Berlin, 1997).
- ⁴L. Mandel and E. Wolf, *Optical Coherence and Quantum Optics* (Cambridge University Press, Cambridge, England, 1995).
- ⁵M.O. Scully and M.S. Zubairy, *Quantum Optics* (Cambridge University Press, Cambridge, UK, 1997).
- ⁶N.H. Bonadeo, J. Erland, D. Gammon, D. Park, D.S. Katzer, and D.G. Steel, *Science* **282**, 1473 (1998).
- ⁷P. Michler, A. Kiraz, C. Becher, W.V. Schoenfeld, P.M. Petroff, L. Zhang, E. Hu, and A. Imamoglu, *Science* **290**, 2282 (2000).
- ⁸C. Santori, M. Pelton, G. Solomon, Y. Dale, and Y. Yamamoto, *Phys. Rev. Lett.* **86**, 1502 (2001).
- ⁹U. Hohenester, F. Troiani, E. Molinari, G. Panzarini, and C. Macchiavello, *Appl. Phys. Lett.* **77**, 1864 (2000).
- ¹⁰F. Troiani, U. Hohenester, and E. Molinari, *Phys. Rev. B* **62**, R2263 (2000).
- ¹¹E. Biolatti, R.C. Iotti, P. Zanardi, and F. Rossi, *Phys. Rev. Lett.* **85**, 5647 (2000).
- ¹²U. Hohenester, *Solid State Commun.* **118**, 151 (2001).
- ¹³A. Zrenner, *J. Chem. Phys.* **112**, 7790 (2000).
- ¹⁴L.C. Andreani, G. Panzarini, A.V. Kavokin, and M.R. Vladimirova, *Phys. Rev. B* **57**, 4670 (1998).
- ¹⁵S.L. McCall and E.L. Hahn, *Phys. Rev. Lett.* **18**, 908 (1967).
- ¹⁶S.L. McCall and E.L. Hahn, *Phys. Rev.* **183**, 457 (1969).
- ¹⁷H.M. Gibbs and R.E. Slusher, *Appl. Phys. Lett.* **18**, 505 (1971).
- ¹⁸R.E. Slusher and H.M. Gibbs, *Phys. Rev. A* **5**, 1634 (1972).
- ¹⁹L. Allen and J.H. Eberly, *Optical Resonance and Two-level Atoms* (Wiley, New York, 1975).
- ²⁰P. Borri, W. Langbein, S. Schneider, U. Woggon, R.L. Sellin, D. Ouyang, and D. Bimberg, *Phys. Rev. Lett.* **87**, 157401 (2001).
- ²¹D. Birkedal, K. Leosson, and J.M. Hvam, *Phys. Rev. Lett.* **87**, 227401 (2001).
- ²²For convenience we use an interaction representation according to $\omega_o \sum_x |x\rangle \langle x| + 2\omega_o |\lambda\rangle \langle \lambda|$.
- ²³H. Haug and S.W. Koch, *Quantum Theory of the Optical and Electronic Properties of Semiconductors* (World Scientific, Singapore, 1993).
- ²⁴See, e.g., P. Yu, W. Langbein, K. Leosson, J.M. Hvam, N.N. Ledentsov, D. Bimberg, V.M. Ustinov, A.Yu. Egorov, A.E. Zhukov, A.F. Tsatsul'nikov, and Yu.G. Musikhin, *Phys. Rev. B* **60**, 16 680 (1999); M. Colocci, A. Vinattieri, L. Lippi, M. Rosa-Clot, S. Taddei, A. Bosacchi, S. Franchi, and P. Friger, *Appl. Phys. Lett.* **74**, 564 (1999).
- ²⁵U. Bockelmann, *Phys. Rev. B* **48**, 17 637 (1993).
- ²⁶L.C. Andreani, G. Panzarini, and J.M. Gérard, *Phys. Rev. B* **60**, 13 276 (1999).
- ²⁷J.M. Gérard, B. Sermage, B. Gayral, B. Legrand, E. Costard, and V. Thierry-Mieg, *Phys. Rev. Lett.* **81**, 1110 (1998).
- ²⁸This corresponds to power densities of a few mW/cm² per pulse.
- ²⁹S.T. Cundiff, A. Knorr, J. Feldmann, S.W. Koch, E.O. Göbel, and H. Nickel, *Phys. Rev. Lett.* **73**, 1178 (1994).
- ³⁰A. Schülzgen, R. Binder, M.E. Donovan, M. Lindberg, K. Wundke, H.M. Gibbs, G. Khitrova, and N. Peyghambarian, *Phys. Rev. Lett.* **82**, 2346 (1999).
- ³¹H. Giessen, A. Knorr, S. Haas, S.W. Koch, S. Linden, J. Kuhl, M. Hetterich, M. Grün, and C. Klingshirn, *Phys. Rev. Lett.* **81**, 4260 (1998).
- ³²Note that because of the mutual light-matter interaction the group velocity depends on the pulse duration, with the tendency of long pulses to travel more slowly than short ones; for details, see, e.g., Ref. 4.
- ³³A. Hartmann, Y. Ducommun, E. Kapon, U. Hohenester, and E. Molinari, *Phys. Rev. Lett.* **84**, 5648 (2000).